UNIVERSITY OF CALIFORNIA SAN DIEGO

Rhythmic Regulation of DNA Methylation by Bmal1 is altered in Alzheimer's Disease

A Thesis submitted in partial satisfaction of the
requirements for the degree Master of Science

in

Biology

by

Arina Alexeeva

Committee in charge:

Professor Paula Desplats, Chair
Professor Nicholas C. Spitzer, Co-Chair
Professor Jose Pruneda-Paz

2018

The Thesis of Arina Alexeeva is approved and it is acceptable in quality and form for publication on microfilm and electronically:

_____

_____

Co-Chair

_____

Chair

University of California San Diego

2018

Dedication

This thesis is dedicated to my parents, Sasha, and Joe for their unconditional love, support and encouragement.

Table of Contents

List of Abbreviations

Aβ	Amyloid-β
AD	Alzheimer's Disease
APP	Amyloid precursor protein
ARH	Adult rat hippocampal neurons
ARN-NPCs	Adult rat hippocampal neural progenitor cells
BMAL1	Aryl hydrocarbon receptor nuclear translocator-like protein 1
CLOCK	Circadian locomotor output cycles kaput
CRY	Cryptochrome
DNMT1	DNA methyltransferase 1
LV-APP	Amyloid precursor protein lentiviral overexpression vector
LV-sGCM	Secreted form of glucocerebrosidase overexpression vector
PER	Period
sGCM	Secreted form of glucocerebrosidase

List of Figures

Acknowledgements

I would like to extend my gratitude to Dr. Paula Desplats for providing me with the opportunity to conduct this work, as well as supporting me throughout its entire process. She has been a truly inspiring role model, both as a scientist and mentor.

I would also like to thank the rest of my committee members, Dr. Nick Spitzer and Dr. Jose Pruneda-Paz, for contributing their valuable time in support of my education.

Finally, I would like to thank all the wonderful members of the Desplats Laboratory who lent their expertise and encouragement during these past two years. Jennifer Mott and Alex Figueroa assisted with the Western Blotting, and Jessica Kim provided valuable help in cell culture.

ABSTRACT OF THE THESIS

Rhythmic Regulation of DNA Methylation by Bmal1 is altered in Alzheimer's Disease

by

Arina Alexeeva

Master of Science in Biology

University of California San Diego, 2018

Professor Paula Desplats, Chair
Professor Nicholas C. Spitzer, Co-Chair

Alzheimer's disease (AD) is on the rise in the U.S. and has no current cure or effective, lasting therapy. AD is associated with circadian and epigenetic disruptions, both of which may contribute to the neurodegeneration, cognitive impairment and dementia characteristic of AD. Epigenetic machinery is known to regulate the circadian clock, however preliminary studies in our lab have suggested that circadian regulators may also regulate epigenetic machinery. We explored the relationship between DNA

methylation and circadian molecular mechanisms in the context of AD. Specifically, we investigated the action of circadian regulator Bmal1 in mediating the expression of DNA methyltransferase 1 (Dnmt1) in rat neurons. We hypothesized that a) Dnmt1 is expressed rhythmically in neurons, that b) Bmal1 acts as a transcription factor to regulate oscillation of *Dnmt1*, and that c) AD pathology alters this rhythmicity and regulation of *Dnmt1*. To generate an *in vitro* model of AD, amyloid precursor protein (APP) was overexpressed in adult rat hippocampal neurons. Dnmt1 transcription in the rat neurons was indeed found to be rhythmic and appeared to be altered in APP-overexpressing neurons. Additionally, we showed that Bmal1 does rhythmically bind to canonical E-boxes present at the *Dnmt1* gene and that this binding is largely reduced with APP-overexpression. Our results not only provide an example of direct circadian control of DNA methylation in neurons, but also support our hypothesis that AD pathology disrupts this regulation. Defining the mechanism behind this relationship may further elucidate the molecular effects of AD pathology, as well as reveal possible circadian targets as future AD therapeutics.

INTRODUCTION

Alzheimer's Disease: Pathology and Clinical Symptoms

Alzheimer's Disease (AD), the most prevalent cause of dementia worldwide, is on the rise in the United States [1, 2]. According to the US Census Bureau, 4.5 million people were affected by AD in the year 2000 and this number is predicted to triple to an alarming 13.2 million by 2050 [2]. The rapid increase in AD is largely due to an expanding group of elderly – the "Baby Boomer" generation – as well as a decline in the death rate of people over 65 years of age [1]. Age is the primary risk factor for AD, with the chance of AD diagnosis doubling every 5 years after the age of 65 [9]. Thus, as the older age group of the US continues to grow and live longer, the incidence of AD is becoming increasingly significant.

Compounded on the rapidly growing prevalence of AD is the fact that there is no current cure or effective lasting therapy for AD. Although there are several available symptomatic treatments, such as cholinesterase inhibitors, none have succeeded in eliminating the symptoms entirely, only halting their progression. Disease modifying drugs, or drugs aiming to stop the course of AD by targeting AD pathology, are still under development and thus not yet available for widespread patient use [7]. This lack of effective treatment options amplifies the critical extent of AD in the U.S.

AD is a neurodegenerative disease that is sporadic, and thus unpredictable, in over 99% of cases (the remaining cases are hereditary, linked to autosomal dominant mutations) [11]. The two primary pathological hallmarks of AD in the brain are extracellular amyloid-β plaques and intracellular neurofibrillary tangles of tau protein.

Amyloid-β (Aβ) is produced via cleavage of the transmembrane amyloid precursor protein (APP) by β-secretase and γ-secretase. The cleavage of APP generates Aβ fragments that are either 40 or 42 amino acids in length (Aβ40 and Aβ42, respectively) [11]. In healthy brains, a certain ratio of Aβ40/Aβ42 is sustained extracellularly, resulting in the formation a low level of amyloid plaques with age. The normal function of Aβ remains unclear, yet Aβ aggregates can be observed in nearly every senile human brain [12]. In AD brains, however, APP is processed improperly, resulting in an inflated production of Aβ42. Aβ42 contains an additional pair of hydrophobic amino acids that enable it to more easily assume the β-sheet conformation and thus aggregate [11]. The aggregated amyloid-β becomes fibrillar over time and it is this fibrillar structure that is believed to be neurotoxic. Fibrillar Aβ plaques recruit and become surrounded by microglia and astrocytes, which in turn stimulate increased expression of inflammatory markers. The up-regulation of inflammatory markers ultimately leads to chronic neuroinflammation, disruption of neuronal function and neuronal death. Moreover, amyloid-β plaques are also known to contain many complement pathway proteins involved in the inflammatory immune response, thus further contributing to chronic neuroinflammation [12].

Compounded on the amyloid-β pathology is the formation of tau neurofibrillary tangles. Tau protein normally mediates microtubule assembly and stabilization. In AD, however, there is an increase in hyper-phosphorylated tau that forms fibrillar tangles in neuronal cell bodies. These intracellular tau tangles correlate with neurodegeneration (independent of Aβ pathology), however the exact mechanisms of tau-induced neuronal death are poorly defined [11].

Clinically, AD manifests as behavioral disruption (such as agitation and altered sleep/wake cycles) cognitive impairment and dementia [13]. The neurodegenerative pathology begins 20-30 years prior to the manifestation of clinical symptoms, and increases in severity with age [12]. Among the most characteristic clinical symptoms of AD is "sundowning", or the increase in AD-related behavioral disturbances (confusion, agitation, cognitive impairment.) in the late afternoon/evening [14]. Sundowning accounts for over 70% of AD patient institutionalizations into care-giving facilities [15]. Sundowning behavior has been shown to correlate with circadian changes: sundowning AD patients have higher nocturnal motor activity and a delayed acrophase of core-body temperature (indicative of a circadian shift) [14]. Furthermore, AD patients are not able to fully synchronize their core-body temperature rhythm with their rest-activity rhythm, indicating a dysfunction of circadian cycling in AD [26]. These time-dependent symptoms associated with sundowning, along with the altered sleep/wake cycles of AD patients, strongly implicate a disruption of the circadian clock in AD [15, 16].

Mammalian Circadian Clock

The circadian clock is present in nearly all light-sensitive organisms, governing both behavioral and physiological processes. In humans, for example, the circadian pacemaker is key to ensuring optimal functioning of metabolism, energy utilization, and detoxification [3]. Circadian machinery is endogenous and regulates 5-10% of the transcriptome, leading approximately 5-20% of all genes to be expressed in a cyclical manner [6]. The organization of the biological clock is hierarchical: the suprachaismatic nucleus (SCN) of the hypothalamus acts as the master clock, the main pacemaker of the

body, and dictates the rhythmicity of peripheral clocks. The SCN is stimulated by environmental light/dark periods via signaling from the optic nerve. Although it was traditionally thought that the SCN controls all peripheral clocks, it is now known that peripheral clocks are capable of functioning in a cell-autonomous manner, thus acting as individual pacemakers [3]. Evidence of this can be seen in *in vitro* models that exhibit circadian oscillations independent of the SCN. For example, fibroblasts in culture have been shown to maintain their own oscillation of circadian proteins without any signaling from the SCN [4]. Furthermore, it is now known that the majority, if not all, cells in the body express the core clock proteins (discussed below) and are therefore able to establish cell-autonomous rhythmicity [6]. In the brain, for example, regions such as the hippocampus, amygdala and frontal cortex exhibit cyclical expression of circadian genes [10, 5].

On a molecular level, circadian rhythmicity in the brain is dictated by oscillations of circadian regulators that act in interlocking positive and negative feedback loops [6]. Nuclear proteins BMAL1 (Aryl Hydrocarbon Receptor Nuclear Translocator-Like Protein 1), CLOCK (Circadian Locomotor Output Cycles Kaput) and NPAS2, an analogue of CLOCK, act as activators in the positive limb of this loop, while the negative regulators Period (PER1-3) and Cryptochrome (CRY1-2) act as repressors in the negative limb [3, 6]. Upon expression, BMAL1 and CLOCK proteins form a heterodimer, that serves as a transcription factor. The heterodimer binds to the E-boxes of *PER1-3* and *CRY1-2* thereby activating their transcription. PER1-3 and CRY1-2 dimerize and translocate into the nucleus where they then hinder the activity of the BMAL1-CLOCK

heterodimer and thus effectively hinder their own transcription. As PER1-3 and CRY1-2 levels fall low, the repression machinery is alleviated and expression of *BMAL1* and *CLOCK* is activated once more [6]. The transcription factor activity of BMAL1 and CLOCK, however, is not solely limited to activation of *PER* and *CRY* genes. Both BMAL1 and CLOCK have been shown to regulate oscillatory expression of many genes and thus modulate biological rhythmicity in the body [8]. The positive and negative feedback loops of the molecular circadian clock are depicted in **Figure 1**.

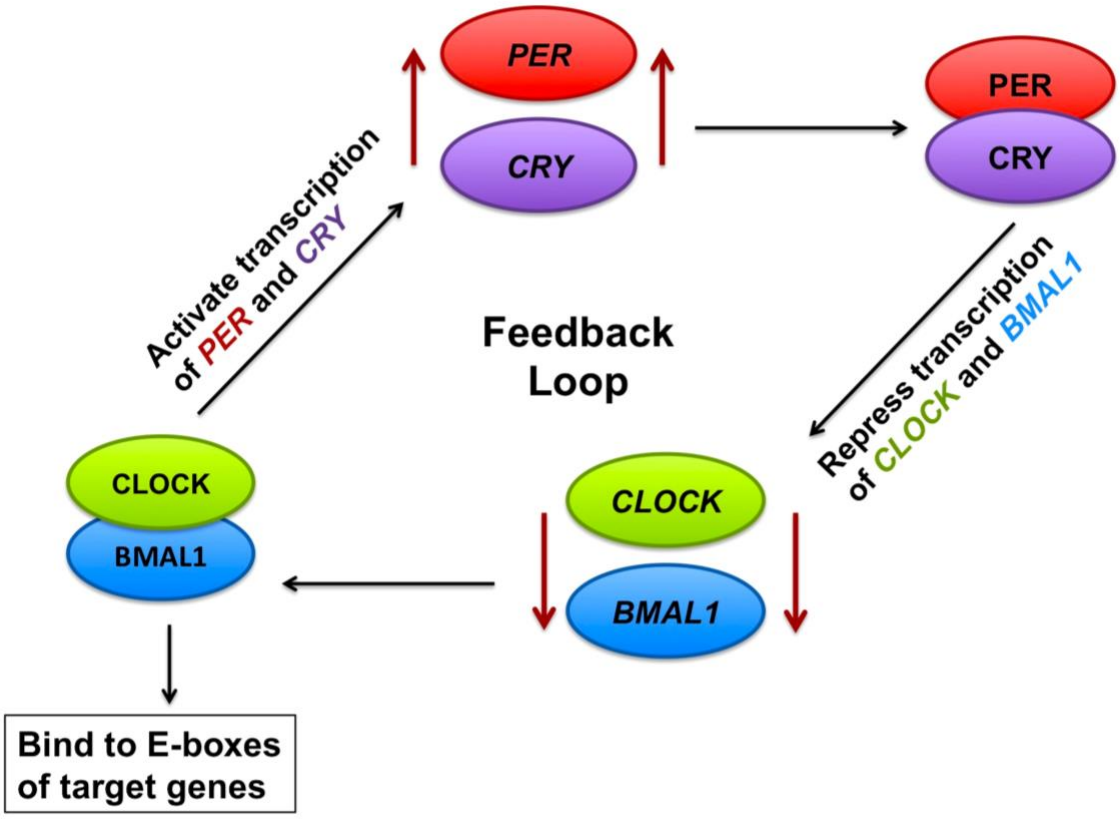

Figure 1. Schematic of major positive and negative circadian regulators.
The positive and negative feedback loops of the molecular circadian clock. Major positive regulators of circadian clock are BMAL1 and CLOCK, major negative regulators are PER and CRY

Rhythmicity of DNA Methylation

The expression of circadian genes is modulated by epigenetic mechanisms, including DNA methylation and histone modifications, and thus it is not surprising that these mechanisms are involved in the regulation of the circadian clock [18-20]. Epigenetic modifications regulate the transcriptional availability of genes, either by inducing changes in chromatin conformation (heterochromatin vs. euchromatin) or by altering the ability of transcriptional machinery to bind at genes' regulatory regions [17]. DNA methylation involves the addition of a methyl group to the cytosine residues in "CpG sites": DNA sequence motifs where a cytosine is followed by a guanine. In mammals, cytosines in CpGs are methylated by DNA methyltransferases (DNMT1, 3a or 3b), which transfer a methyl group from S-adenosyl-L-methionine to DNA cytosine. Methylated CpG sites hinder the binding of transcription factors and initiate a heterochromatic state, thus decreasing transcriptional availability of neighboring genes and effectively repressing gene expression [17].

DNA methylation has been shown to regulate expression of core circadian proteins. The regulatory regions of several circadian clock genes are known to contain significantly more CpG motifs as compared to other genes [19]. In mouse SCN and liver cells, *Per2* is methylated at 4 CpG sites within its promoter region. Moreover, this methylation was demonstrated to inhibit expression of *Per2* [20]. In vivo, mice exposed to altered light:dark cycles (22 or 26-hours instead of 24-hours) exhibited altered DNA methylation in the SCN. Mice housed in abnormal light cycles (22 or 26 hours) were found to have altered methylation at 1,294 DNA, CpG sites as compared to the 24-hour light period control mice. These 1,294 regions included the promoters of several clock

genes: *Per2*, *Cry1* and *Clock*. Furthermore, the altered light-period mice also showed changes in global transcription levels in the SCN. Specifically, for instance, the peak and nadir of circadian gene expression changed in correlation with the altered methylation of their promoters [21]. The findings above not only demonstrate the direct role of DNA methylation in regulating circadian genes, but also suggest DNA methylation as a driver of circadian clock plasticity.

Given DNA methylation's possible role in circadian plasticity, it is not surprising that DNA methylation in the human brain has been shown to rhythmically cycle. Lim et. al (2014) show that the methylation of multiple CpG sites across the genome and located near transcription start sites cycles with 24-hour rhythmicity in the human prefrontal cortex. Furthermore, this 24-hour DNA methylation cycling precedes the expression of nearby genes by 1-3 hours [22]. Cronin et. al (2016) specifically examined the relationship between such 24-hour methylation rhythms and the expression of a main circadian regulator: *BMAL1*. Analysis of post-mortem human midfrontal cortices by methylation array revealed intermediate levels of methylation at the 5'-untranslated region (5' UTR) of *BMAL1*. Using the time of death as a function of circadian time, the authors demonstrated that CpG sites in *BMAL1*'s 5'UTR are rhythmically methylated. Furthermore, the abundance of *BMAL1* transcript correlated with the methylation some of the CpG in *BMAL1*'s 5'UTR [23]. These findings suggest a direct relationship between *rhythmic* DNA methylation and expression of core circadian regulator *BMAL1*, as well as support circadian-like cycling of DNA methylation.

Disruptions of Circadian Machinery and DNA Methylation Rhythmicity in AD

AD is associated with significant disruptions of both circadian rhythmicity and DNA methylation in the brain. Sundowning and fragmented sleep/wake cycles, as previously discussed, are characteristic symptoms of AD and are highly indicative of disruptions in circadian machinery [15, 16]. Cronin et. al (2016) examined circadian abnormalities in AD by quantifying *BMAL1* levels in fibroblasts derived from AD patients and in frontal cortices of post-mortem AD patients. Both in vitro and in vivo, *BMAL1* transcript and protein levels are significantly altered with AD pathology. AD fibroblasts exhibited a delayed expression peak, significant phase advance and alterations in cycle amplitude and period of *BMAL1* transcript as compared to fibroblasts derived from healthy subjects [23]. Similarly, in the frontal cortex of AD patients, *BMAL1* had an advanced phase of transcription and lower amplitude of transcript abundance in comparison to healthy controls. BMAL1 protein levels in AD patient brains peak in the morning, while BMAL1 protein in healthy brains peaks in the evening [23]. Combined together, these findings point to a significant disruption in the cycling of circadian protein *BMAL1* in AD pathology.

To analyze the possible role of DNA methylation in these circadian alterations, Cronin et. al (2016) also examined the methylation of *BMAL1* in AD brains. The authors had previously demonstrated, as discussed above, that there is cyclic DNA methylation at *BMAL1*'s 5'UTR in healthy brains. Methylation array showed that methylation peak times at *BMAL1*'s 5'UTR are altered in AD brains, as compared to healthy control brains. In particular, for example, five CpG sites in *BMAL1*'s 5'UTR reached their methylation peak simultaneously and this methylation peak was in complete anti-phase between AD

and healthy subjects. To analyze if DNA methylation directly affected *BMAL1* transcription, the authors inhibited DNA methyltransferases (DNMTs) in healthy and AD derived fibroblasts and quantified levels of *BMAL1*. Inhibition of DNMTs yielded concentration dependent changes in period length, phase and amplitude of *BMAL1* both in control and AD cells [23]. Taken together these findings evidence a disruption in cyclic DNA methylation with AD, particularly in the rhythmic methylation of circadian protein *BMAL1*.

The presence of both circadian and epigenetic disruptions in AD brings up the question of how these two mechanisms are related in AD pathology. The data presented above suggests an epigenetic driven disruption of the circadian clock: changes in DNA methylation rhythmicity are associated with changes in *BMAL1* oscillation. However, there is also potential for a circadian driven disruption in DNA methylation rhythmicity. Preliminary studies in our laboratory (Desplats Laboratory at the UCSD Department of Neuroscience) have uncovered several canonical binding sites for BMAL1 circadian protein on the promoter of several DNA methyltransferases (*DNMT*s). Furthermore, RNA-sequencing of about 400 post-mortem brain samples from the Religious Order Study (ROS) and the Memory Aging Project (MAP) – the largest studies on aging in the U.S. – revealed that *DNMT1* is the most abundant DNA methyltransferase isoform in the cortex and shows oscillatory expression. These preliminary findings demonstrate the potential of BMAL1 to act as a transcription factor in regulating the expression of *DNMT*s. We hypothesized that the circadian disruptions of *BMAL1* in AD directly alter expression of *DNMT*s. Specifically; we examined how the accumulation of amyloid- β influences the expression of *Dnmt1*. Consequently, we investigated if Bmal1 does indeed

act as a transcription factor to *Dnmt1* and (if so) how the time-dependent recruitment of Bmal1 to *Dnmt1's* promoter is disrupted by accumulation of amyloid- β. We hope this project will elucidate the mechanism linking the circadian clock to epigenetics in AD and thus open the possibility of targeting circadian proteins in future AD treatments.

MATERIALS AND METHODS

Cell Culture: Adult Rat Hippocampal Neurons

Adult rat hippocampal neural progenitor cells (ARH-NPCs) were cultured in DMEM/F12 without HEPES, supplemented with 2mM L-glutamine, 100 U/mL Penicillin-Steptomycin, B27 without vitamin A, and 20ng/mL of fibroblast growth factor (FGF) 2. The cells were grown on plates coated with poly-L-Ornithine and Laminin. The ARH-NPCs were infected with lentivirus overexpressing human wild type amyloid precursor protein (APP) to generate an in vitro neuronal model of Alzheimer's disease. Control ARH-NPCs were infected with lentivirus carrying the secreted form of glucocerebrosidase (sGCM) in the same backbone. This control was chosen to ensure that changes seen with APP overexpression are not due to overexpression and exporting of a foreign protein. Two days post infection the control (CT) and APP-overexpressing ARH-NPCs were differentiated into ARH neurons for 4 days in differentiation media. Differentiation media consisted of DMEM/F12 without HEPES, supplemented with 2mM L-Glutamine, 100 U/mL Penicillin-Steptomycin, B27 without Vitamin A, 1uM Retinoic Acid, 5uM Forskolin and 1% Fetal Bovine Serum. Successful differentiation was assessed by presence of neuronal projections (**Figure 2**). On the 4th day of differentiation cell processes were synchronized with 2X Forskolin (10uM). Control and APP-overexpressing ARH neurons were collected every 6 hours starting 36 hours post synchronization. Cells were flash frozen during collection to stop cell processes simultaneously.

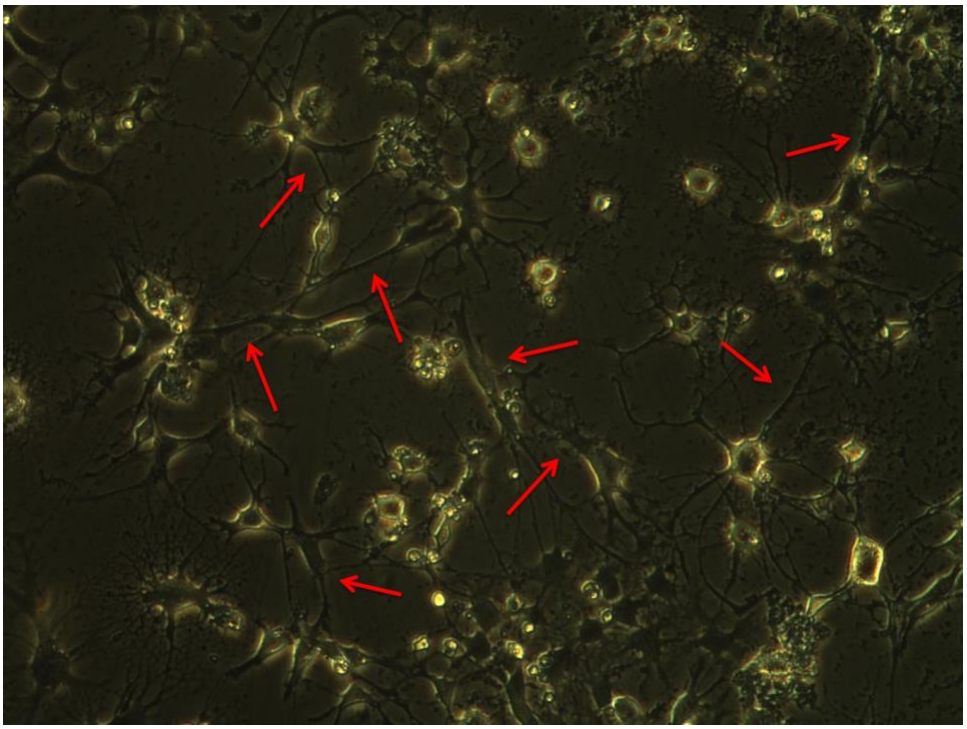

Figure 2. 4-day differentiated adult rat hippocampal neurons (ARH neurons). ARH neural progenitor cells were cultured in media supplemented with 1uM Retinoic Acid and 5uM Forskolin for 4 days to stimulate differentiation into neurons. Red arrows indicate neuronal projections indicative of differentiation.

Cell Culture: Bmal1 Knockout (Bmal1 KO) Fibroblasts

A Bmal1 knockout (Bmal1 KO) fibroblast line was established from the tails of four heterozygous Bmal1 knockout mice (strain B6.129-*Arntl*^{tm1Bra}*IJ*, generously donated by the Welsh Lab), according to previously published protocols [35].

The Bmal1 KO fibroblasts and NIH3T3 fibroblasts (for control) were cultured in DMEM media with 4.5g/L Glucose, Sodium Pyruvate supplemented with 2mM L-glutamine, 100 U/mL Penicillin-Streptomycin, and 1X Gibco MEM Non-essential Amino Acids. Fibroblasts were harvested for downstream analysis.

Bmal1 reduction in the Bmal1 KO fibroblasts was corroborated at the mRNA level via real-time PCR (qPCR) using TaqMan Gene Expresson Assays (Applied Biosystems). The Bmal1 KO fibroblasts had a 50% reduction in *Bmal1* transcripts, compared to control NIH3T3 cells (**Figure 3**). Bmal1 reduction was also corroborated at the protein level via NuPAGE 3-8% Tris-Acetate gel (Invitrogen) probing with Bmal1 antibody (sc-365645 1:100 dilution in 5% BSA PBS-Tween) (**Figure 4A**). Densitometry analysis revealed an 89% reduction in Bmal1 protein abundance in the Bmal1 KO fibroblasts compared to NIH3T3 fibroblasts (**Figure 4B**). A paired, two-tailed t-test by was used to analyze real-time PCR fold change results of Bmal1 KO fibroblasts.

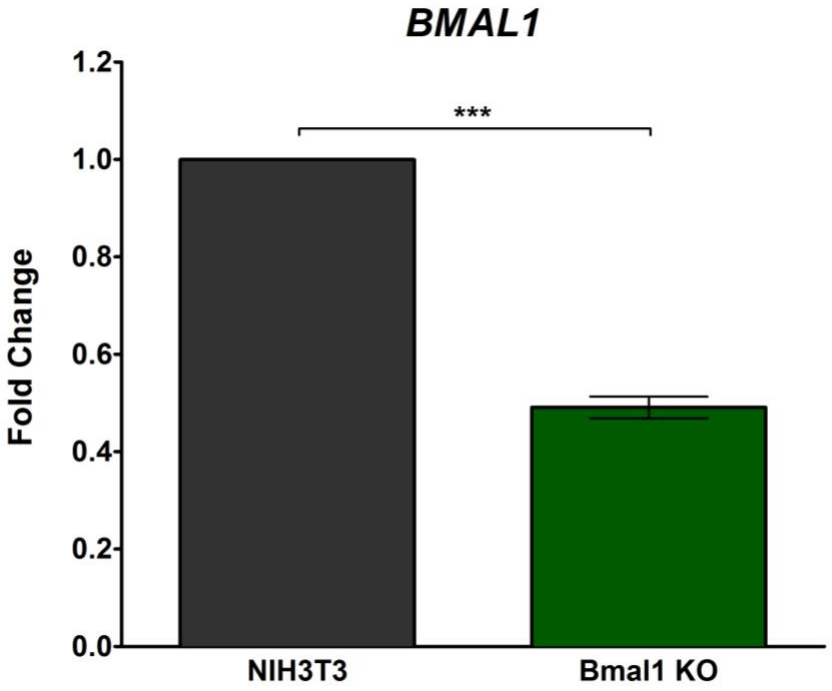

Figure 3. *Bmal1* mRNA is decreased in the Bmal1 knockout (Bmal1 KO) fibroblast line. Real-time PCR to quantify Bmal1 in the Bmal1 knockout (Bmal1 KO) fibroblast line and NIH3T3 fibroblast line ($p<0.0002$, $n=4$).

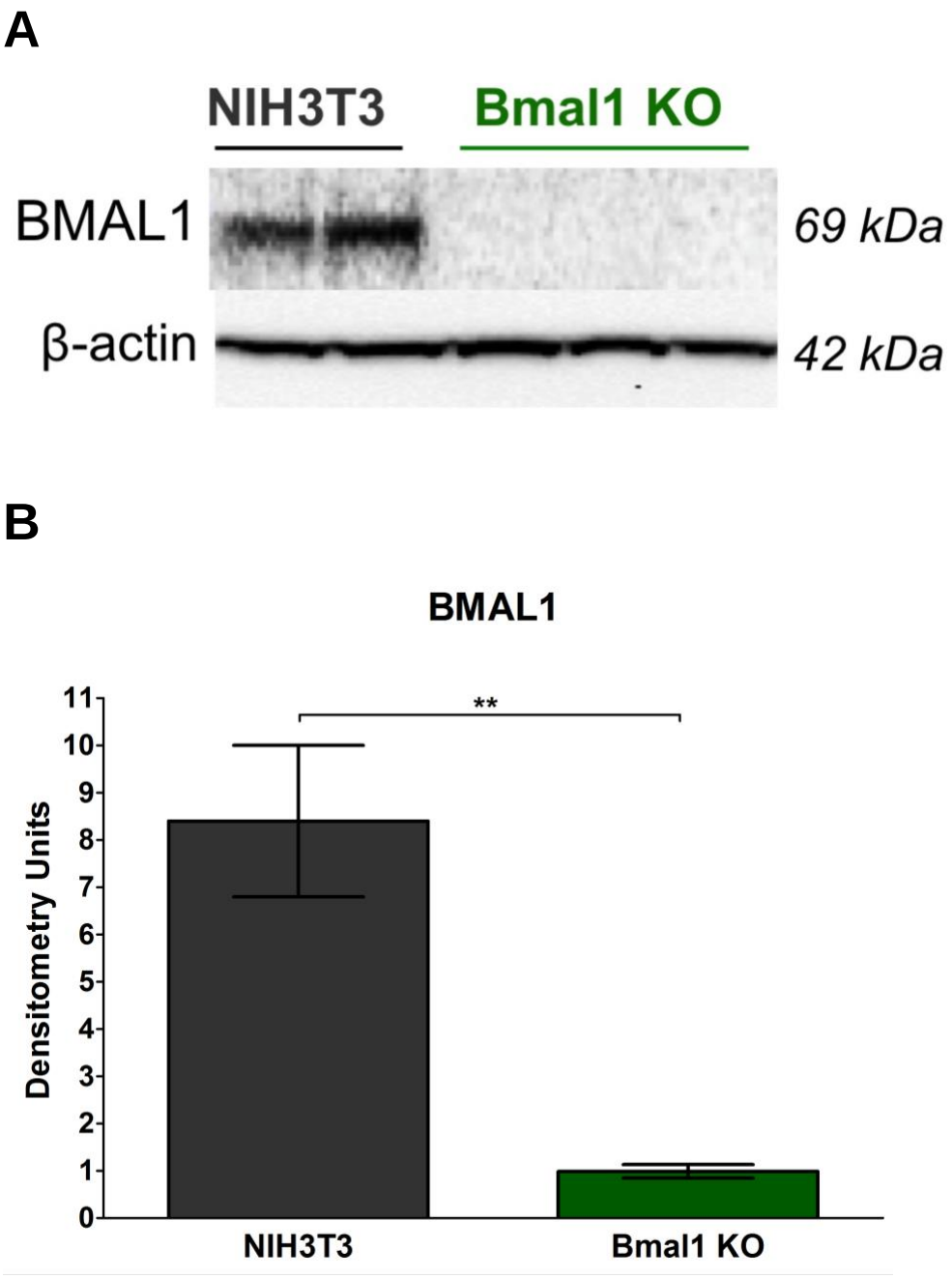

Figure 4. Bmal1 protein is decreased in the Bmal1 knockout (Bmal1 KO) fibroblast line.
A) Western blot of protein isolated from the Bmal1 KO fibroblasts and control NIH3T3 fibroblasts. Blot was probed with antibody to visualize Bmal1 (~69kDa) **B)** Densitometry to quantify Bmal1 protein in the Western Blot from (B), with the two NIH3T3 lines grouped and the three Bmal1 KO fibroblast lines grouped ($p=0.0087$ with $n=3$).

Immunoprecipitation of Amyloid-β from Culture Media

To verify that the APP ARH neurons were able to process and export the overexpressed human APP into extracellular amyloid-β, culture media from 4-day differentiated ARH neurons was assessed for amyloid-β levels. Differentiation media from control and APP ARH neurons was collected on the 4th day of differentiation and 1X EDTA free Protease Inhibitor Cocktail Set III (Calbiochem) was added to the media. Amyloid-β was immunoprecipitated from the collected media with Protein G Dynabeads (novex by Life Technologies) using 20ug of amyloid-β 6E10 antibody (BioLegend) per 2mL of culture media. Immunoprecipitated amyloid-β was resuspended in PBS with 1X NuPAGE LDS Sample Buffer and NuPAGE Sample Reducing Agent (Thermo Fischer), boiled at 70°C for 10 minutes, and ran on an NuPAGE 4-12% Bis-Tris protein gel (Thermofischer) in NuPAGE MES SDS running buffer (Thermo Fischer). Dry gel transfer was done via the iBLOT2 Gel Transfer Device from Thermo Fischer and amyloid-β detected with 6E10 amyloid-β antibody (BioLegend) diluted 1:1000 in 5% BSA PBS-Tween.

Real-Time PCR (qPCR)

RNA was extracted from collected ARH neurons, Bmal1 KO fibroblasts and NIH3T3 fibroblasts using RNeasy Plus Mini Kit (QIAGEN). 500ng-1ug of RNA was converted to cDNA with the High Capacity cDNA Reverse Transcriptase Kit (Applied Biosystems). Levels of mRNA were quantified by real-time PCR (qPCR) using TaqMan Gene Expression Assays (Applied Biosystems) with TaqMan Fast Master Mix and TaqMan Gene Expression Assay primers: rat *Bmal1, Dnmt1, Per2, β –Actin* and human

APP for ARH neurons' mRNA. Mouse *Bmal1*, *Dnmt1* and *β –Actin* primers were used for Bmal1 KO and NIH3T3 fibroblasts' mRNA. StepOnePlus Real-Time PCR System with StepOne Comparative Ct Software was used to quantify Ct values. Relative quantification of transcript abundance was calculated by the Double Delta Ct method.

Western Blot

1X RIPA Buffer (Cell Signaling) supplemented with EDTA free Protease Inhibitor Cocktail Set III and Phosphatase Inhibitor Cocktail Set III (Calbiochem) was used to extract protein from collected ARH neurons, Bmal1 KO fibroblasts and NIH3T3 fibroblasts. Protein concentration was quantified via BCA assay (Thermo Fischer).

Protein extracts were ran on NuPAGE 4-12% Bis-Tris or NuPAGE 3-8% Tris-Acetate gels (Invitrogen) using 1X MES SDS Running Buffer or 1X Tris Acetate SDS Running Buffer (Novex Life Technologies), respectively. Gels were equilibrated in 20% ethanol for 5 minutes at room temperature. Immunoblots were transferred via iBLOT2 (Thermo Fischer) using a modified protocol for transfer of high molecular weight proteins: 1 minute at 20V, 2 minutes at 23V and 4 minutes at 25V. Blots were blocked with 5% BSA in PBS-Tween. Immunoblots were probed for Bmal1 (abcam 140464 1:1000 dilution or sc-365645 1:100 dilution in 5% BSA PBS-Tween), Dnmt1 (abcam 188453 1:1000 dilution in 5% BSA PBS-Tween), β-Actin (BioLegend 6E10 1:1000 dilution in 5% BSA PBS-Tween). Developing and densitometry was done with VersaDoc and Quant-IT Image Studio software (BioRad).

ChIP-IT High Sensitivity Assay

LV-APP and LV-sGCM infected ARH-NPCs were differentiated for 3 days and synchronized with 2X Forskolin on the 3rd day of differentiation, as previously described (*Cell Culture: Adult Rat Hippocampal Neurons*). Cells were fixed with 37% formaldehyde, according to the ChIP-IT High Sensitivity protocol by Active Motif, and collected at 6 and 12 hours post the 36 hours synchronization. Formaldehyde fixation acted to cross-link DNA-protein complexes in the cells to maintain complexes for downstream ChIP immunoprecipitation. Approximately $2x10^7$ control neurons and $2x10^7$ APP-overexpressing ARH neurons were collected at each timepoint. At each timepoint, a portion of the ARH neurons were collected without ChIP-IT formaldehyde fixation for mRNA analysis (described below).

To determine the peak and nadir of Bmal1 expression in the collected ARH neurons, *Bmal1* mRNA levels were quantified with qPCR using TaqMan Gene Expression Assays (Applied Biosystems). TaqMan Fast Master Mix and TaqMan Gene Expression Assay primers were used: rat *Bmal1* and *β –Actin.* StepOnePlus Real-Time PCR System with StepOne Comparative Ct Software was used to quantify Ct values. $1/\Delta Ct$ was calculated using *β –actin* for normalization and values were plotted against hours post synchronization with PRISM Software to see the peak and nadir of Bmal1 expression. *Bmal1* expression was at a nadir at 0 hours post synchronization and peaked 12 hours post synchronization. Control and APP ARH neurons fixed and collected at these two timepoints were selected for downstream ChIP-IT analysis.

ChIP-IT was performed on selected control and APP ARH neurons according to the vendor protocol (Active Motif: cat# 53040). Cell lysis and chromatin shearing was

done with dounce homogenization and 10 minutes of sonication per sample. Chromatin shearing was confirmed with gel electrophoresis (**Figure 5**). Immunoprecipitation was done with rat Bmal1 antibody (ab3350, 4ug). IgG antibody (sc-2027 and sc-2025) and RNA Polymerase II antibody were used as immunoprecipitation controls.

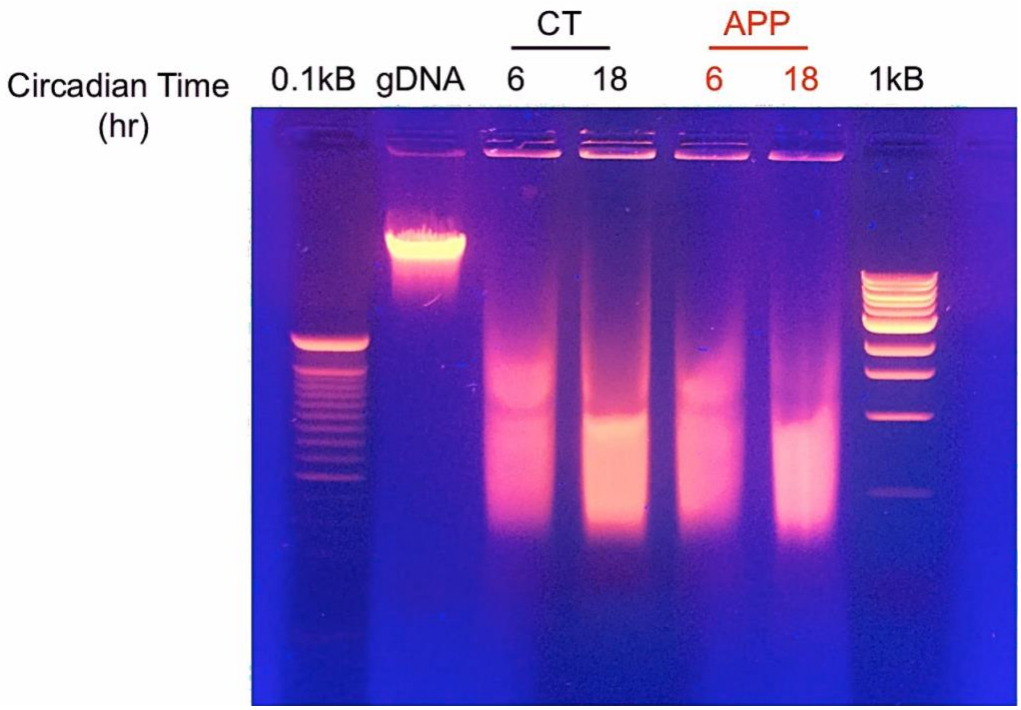

Figure 5. Chromatin shearing of adult rat hippocampal neurons for ChIP. Sheared chromatin from control (CT) and APP-overexpressing (APP) adult rat hippocampal neurons collected at 6 and 18 hours post fixation (indicated as circadian time). Genomic DNA from 293T human embryonic kidney cells (gDNA) was ran as control for intact chromatin.

ChIP chromatin analysis was done via qPCR using 2X Power SYBER Green PCR Master Mix (Applied Biosciences) and primers flanking the three canonical binding sites (E-boxes 1-3) for Bmal1 on rat *Dnmt1* promoter. E-box 1 is 1462bp upstream of *Dnmt1*

coding sequence, E-box 2 is 1361bp upstream of *Dnmt1* coding sequence, and E-box 3 is 383bp upstream of *Dnmt1* coding sequence. Negative control primers were designed to anneal 10-20kB upstream of the rat *Dnmt1* promoter. Positive control rat primers flanked known Bmal1 targets on *Per2* and *Dbp* promoters.

Real-Time PCR Data Analysis

To analyze the time-dependent transcript abundance, the inverse of the Delta in cycle threshold between *Bmal1* or *Dnmt1* and *Actin* was calculated first. Relative abundance was then normalized by assigning 100% abundance to the highest 1/ΔCt value in the series. Relative abundance versus hours post synchronization of cell processes was plotted. Time 0 was assigned to neurons collected at 36 hours of synchronization of cell processes. The oscillation of *Bmal1*/*Per2* was normalized with a LOWESS fit curve.

The real-time PCR of the Bmal1 KO fibroblast and NIH3T3 fibroblast cDNA was analyzed by calculating 1/ΔCt using *β –Actin* for normalization and plotting *Bmal1* 1/ΔCt versus *Dnmt1* 1/ΔCt. The correlation between *Bmal1* and *Dnmt1* abundance was determined by Pearson's r using PRISM GraphPad Software. Fold change was calculated using NIH3T3 fibroblasts as reference and statistical significance was determined with paired, two-tailed t-test by PRISM GraphPad Software.

For the analysis of Bmal1 binding to the *Dnmt1* promoter, qPCR data obtained from the precipitated chromatin was adjusted to the primer calculated efficiency. Fold enrichment was calculated in relation to total chromatin pulled down with the IgG antibody. Primer efficiency was calculated using serial dilutions of input chromatin. One-way Anova with Bonferroni's Multiple Comparisons post-hoc test (in PRISM GraphPad

Software) was used to assess differences in fold enrichment in Bmal1 -precipitated chromatin at different time points in CT and APP neurons.

Western Blot Data Analysis

Densitometry was done with VersaDoc and Image Studio Software. Obtained protein levels were normalized to β-Actin levels and densitometry units converted to a 0-10 scale by assigning the highest densitometry units to a value of 10. An unpaired, two-tailed t-test by PRISM GraphPad Software was used to determine statistical significance of densitometry analysis.

RESULTS

Alzheimer's Disease Model

To create an in vitro neuronal model of Alzheimer's disease, adult rat hippocampal neural progenitor cells (ARH-NPCs) were infected with lentivirus to overexpress human amyloid precursor protein (APP). Improper processing of APP by β-secretase and γ-secretase is a characteristic hallmark of Alzheimer's pathology, resulting in the accumulation of extracellular amyloid-β (Aβ) plaques in the brain [11]. The infected ARH-NPCs were differentiated for 4 days into ARH neurons (**Figure 6**). To ensure that APP was successfully overexpressed, levels of APP mRNA and protein were quantified via qPCR and Western Blot, respectively. APP infected ARH neurons had a $9x10^5$ fold increase in APP expression compared to control ARH neurons (**Figure 7A**). Similarly, Western Blot analysis confirmed the overexpression of APP protein in APP-overexpressing neurons compared to control neurons (**Figure 7B**). Quantification of protein levels via densitometry indicated a 13-fold increase in APP with its overexpression (**Figure 7C**).

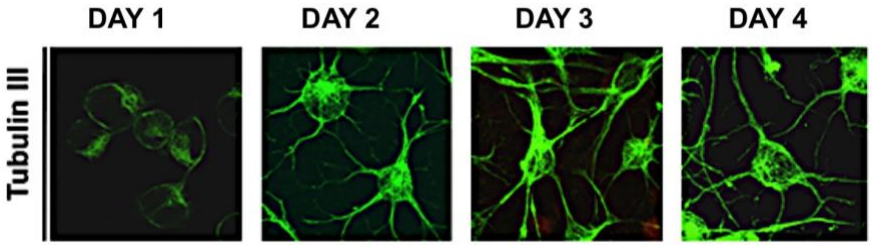

Figure 6. Adult rat hippocampal (ARH) neuron differentiation.
Adult rat hippocampal neural progenitor cells (ARH-NPCs) differentiated for 4 days into adult rat hippocampal neurons (ARH neurons). ARH-NPCs were differentiated with 1uM retinoic acid and 5uM Forskolin supplement in culture media.

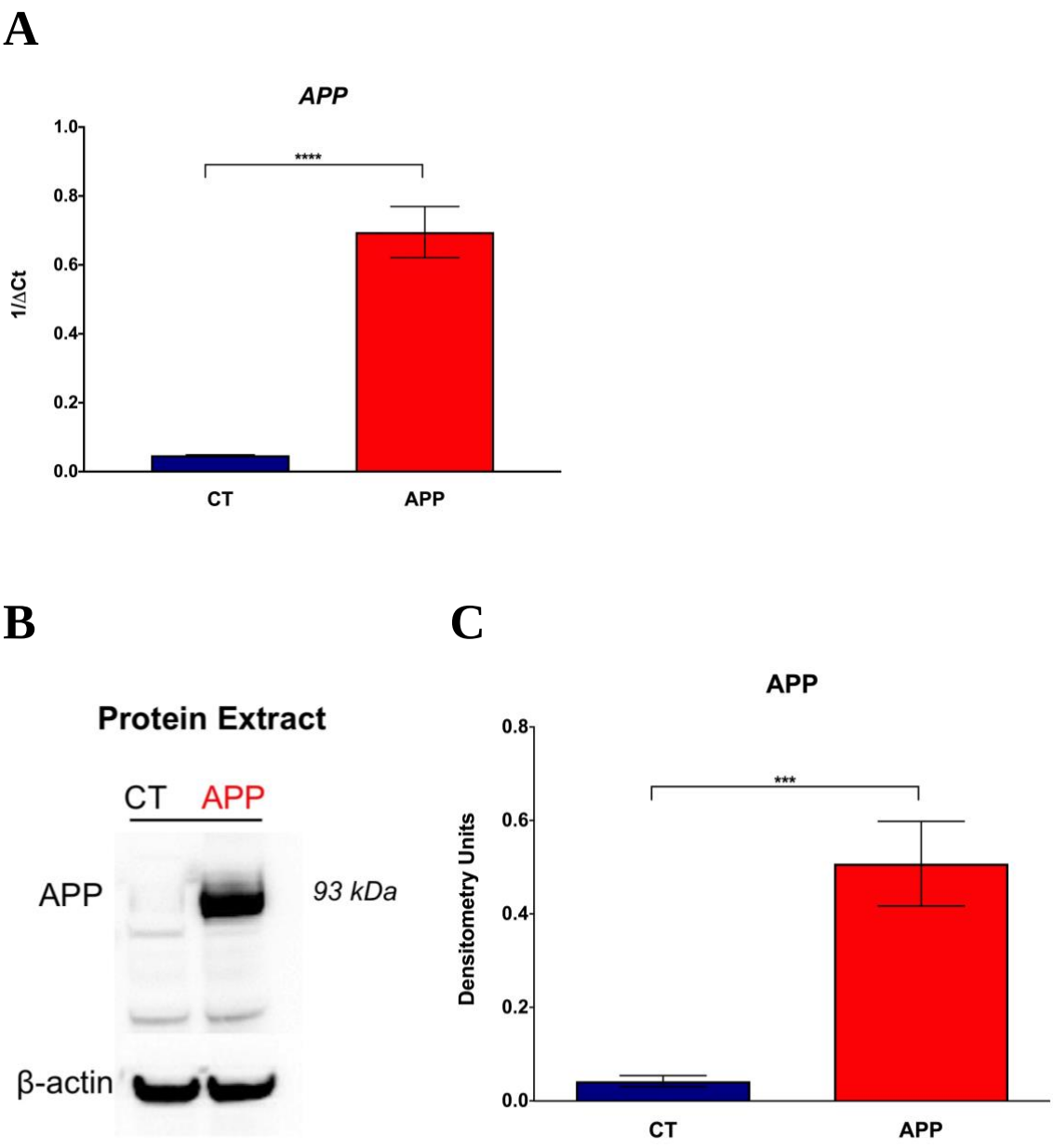

Figure 7. Overexpression of amyloid precursor protein (APP) in adult rat hippocampal neurons (ARH neurons).
A) qPCR to quantify abundance of *APP* in APP-overexpressing (APP) versus control (CT) ARH neurons ($p<0.0001$ with n=3) **B)** Western Blot of protein extract from control (CT) versus APP-overexpressing (APP) ARH neurons. Blot was stained with antibody against APP (6E10) to visualize APP protein (~93kDa). **C)** Densitometry to quantify APP protein in Western Blot from *(B)*, and two other biological replicates ($p<0.0002$ with n=3).

To ensure that the APP-overexpressing ARH neurons were not only expressing but also cleaving and exporting APP into extracellular amyloid-β (Aβ), as is characteristic in Alzheimer's pathology, we assessed the culture media of the ARH neurons for the presence of Aβ-fragments. We used an antibody against Aβ to immunoprecipitate Aβ from the culture media of APP-overexpressing and control ARH neurons. Immunoprecipitated media was ran on a Western Blot and probed for Aβ. Western Blot analysis indicated high levels of Aβ-fragments in the media of APP-overexpressing ARH neurons, but very low levels in the media from control neurons (**Figure 8A**). Densitometry revealed a 1.5 fold increase in extracellular Aβ in the media of APP-overexpressing ARH neurons compared to control neurons (**Figure 8B**).

To ensure that our in vitro Alzheimer's model exhibited the circadian disruptions previously reported in Alzheimer's pathology, specifically in the rhythmicity of circadian regulator Bmal1, we assessed a) whether the ARH neurons expressed Bmal1 cyclically, and b) whether the rhythmicity of Bmal1 expression was altered by APP-overexpression. Levels of *Bmal1* expression were evaluated via qPCR in cells collected every 6 hours after synchronization. The control ARH neurons were indeed found to express *Bmal1* rhythmically: *Bmal1* mRNA levels peaked every 20-24 hours (**Figure 9A**). Moreover, *Bmal1* expression was anti-phasic to the expression of circadian regulator *Per2*, which is consistent with previous reports [6] of *Bmal1* and *Per2* rhythmicity (**Figure 9B**). In the APP-overexpressing ARH neurons, however, the oscillation of *Bmal1* was aberrant. Compared to control neurons, the APP-overexpressing neurons showed an advanced phase of *Bmal1* transcription with fragmented patterns (**Figure 9A**). To examine the rhythmicity of Bmal1 protein, we quantified Bmal1 protein abundance by Western Blot

in control and APP-overexpressing ARH neurons, collected at 0 and 12 hours. Bmal1 protein differing levels between time-points, both in control and APP-overexpressing neurons (**Figure 10A**). Moreover, the APP-overexpressing neurons had dampened levels of Bmal1 protein at each time-point, compared to control neurons (**Figure 10A**), in agreement with previous reports of increased Bmal1 degradation in AD models [36]. Compiled densitometry of Bmal1 protein from three independent experiments confirmed this time-dependent change in Bmal1 abundance: Bmal1 levels decreased over the course of 12 hours both in control and APP-overexpressing neurons (**Figure 10B**). The decrease in Bmal1 abundance in APP-overexpressing neurons was also confirmed via densitometry: the APP-overexpressing neurons had 33% less Bmal1 protein at 0 hours and 45% less Bmal1 protein at 12 hours, compared to control neurons (**Figure 10B**).

A

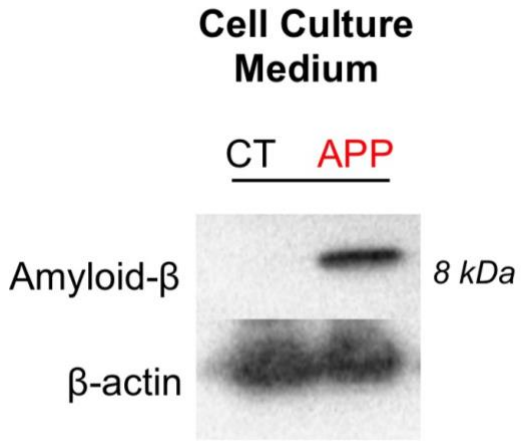

B

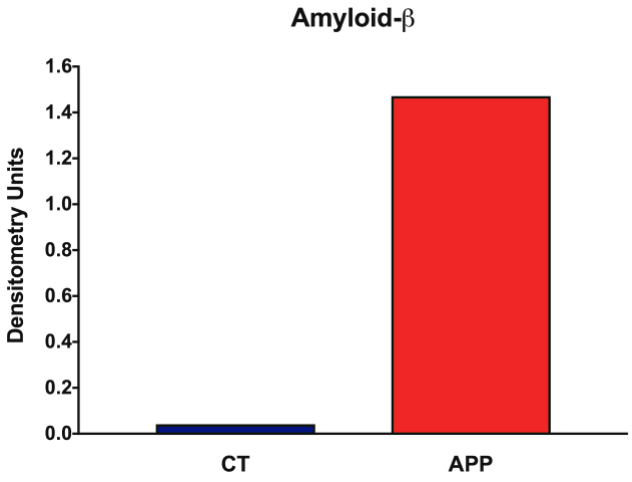

Figure 8. **Amyloid-β (Aβ) in culture media of APP-overexpressing ARH neurons.** **A)** Western Blot of protein immunoprecipitated from the culture media of APP-overexpressing (APP) and control (CT) ARH neurons. Immunoprecipitation was done with Aβ antibody (6E10). Blot was stained with 6E10 antibody to visualize Aβ protein (~8kDa). **B)** Quantification of Aβ in Western Blot from *(B)* by densitometry.

A

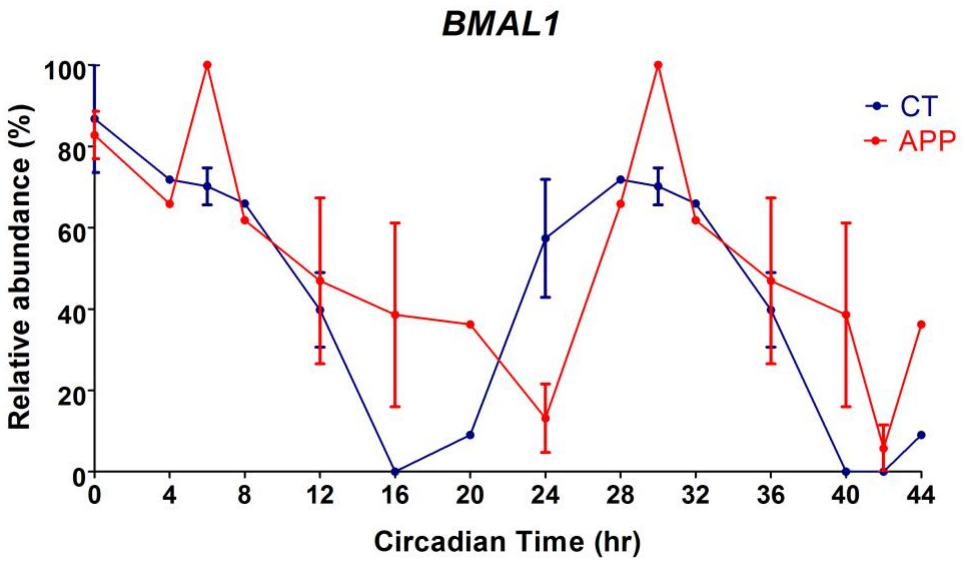

B

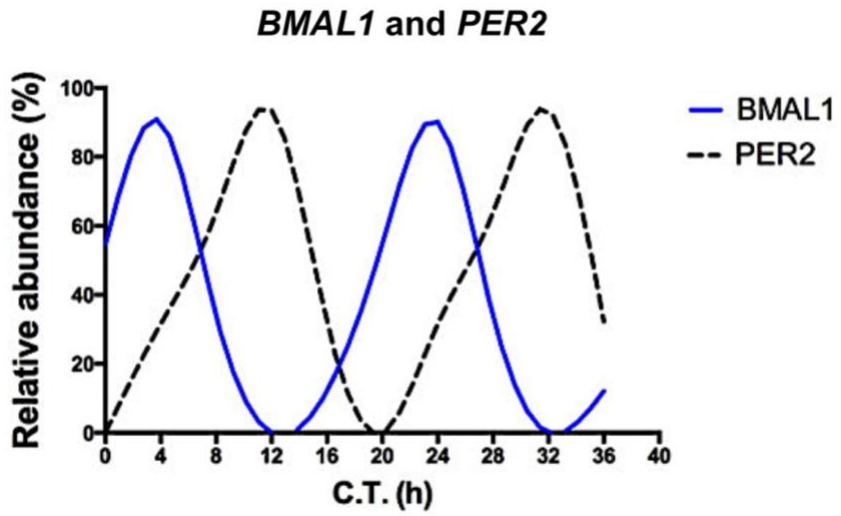

Figure 9. *Bmal1* is expressed rhythmically in adult rat hippocampal (ARH) neurons and exhibits aberrant rhythmicity with APP-overexpression.
A) Real-time PCR to quantify relative abundance of *Bmal1* in APP-overexpressing (APP) versus control (CT) ARH neurons over time. Relative abundance determined by assigning 100% abundance to the highest 1/ΔCt value. Graph shows compiled data from four biological replicates. **B)** Real-time PCR to quantify relative abundance of *Bmal1* and *Per2* in control (CT) ARH neurons over time. LOWESS fit curve was applied.

A

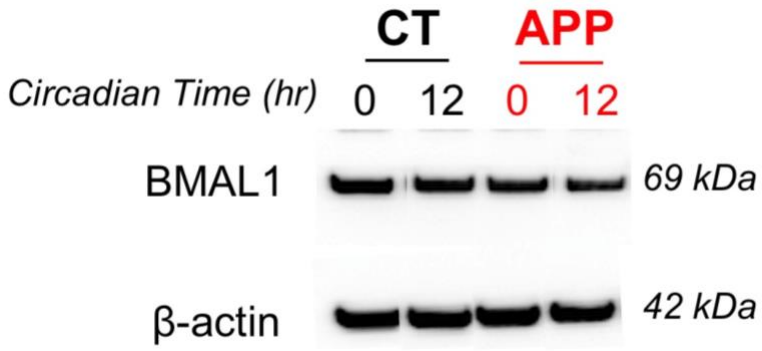

B

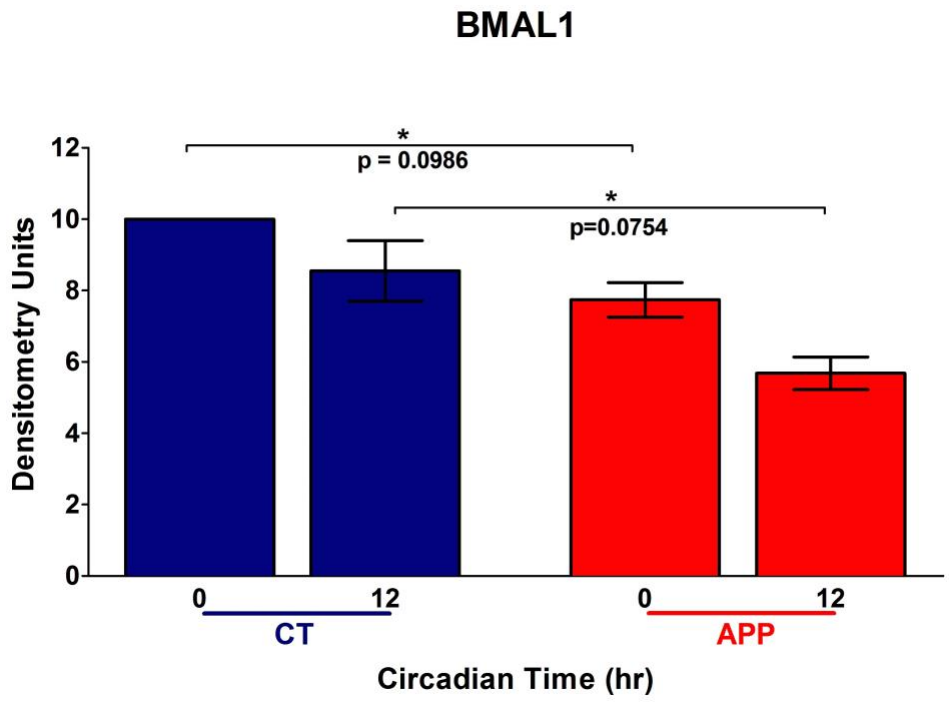

Figure 10. Bmal1 protein levels are rhythmic in ARH neurons and Bmal1 abundance is dampened with APP-overexpression.
A) Western Blot of protein extract from control (CT) versus APP-overexpressing (APP) ARH neurons, collected every 6 hours post synchronization. Blot was probed with antibody to visualize Bmal1 (~69kDa). **B)** Densitometry to quantify Bmal1 protein in Western Blot from *(B)*, and two other biological replicates at 0 and 12 hours post 36-hour synchronization (n=3).

Dnmt1 Rhythmic Expression

To investigate whether DNA methyltransferase 1 (Dnmt1) exhibits circadian like rhythmicity in neurons and, if so, whether this rhythmicity is altered with amyloid-β accumulation, we examined Dnmt1 expression in control and APP-overexpressing ARH neurons. Levels of *Dnmt1* were evaluated via qPCR in cells collected every 6-hours after synchronization. We observed rhythmic transcription of *Dnmt1* in control neurons (**Figure 11**). In the APP-overexpressing ARH neurons, the oscillation of *Dnmt1* was aberrant, and shows advanced phase (**Figure 11**). To examine the potential oscillation of Dnmt1 protein we quantified protein levels in control and APP-overexpressing ARH neurons, collected every at 0 and 12 hours by immunohistochemistry. Dnmt1 protein levels differed between 0 and 12 hours, both in control and APP-overexpressing neurons (**Figure 12A**). Moreover, the APP-overexpressing neurons appeared to show inversed patterns of Dnmt1 protein expression in comparison to control neurons (**Figure 12A**). Compiled densitometry of Dnmt1 protein from three independent experiments confirmed this time-dependent change: Dnmt1 levels increased by 38% from 0 to 12 hours in control neurons, but decreased by 32% in the same period in APP-overexpressing neurons (**Figure 12B**).

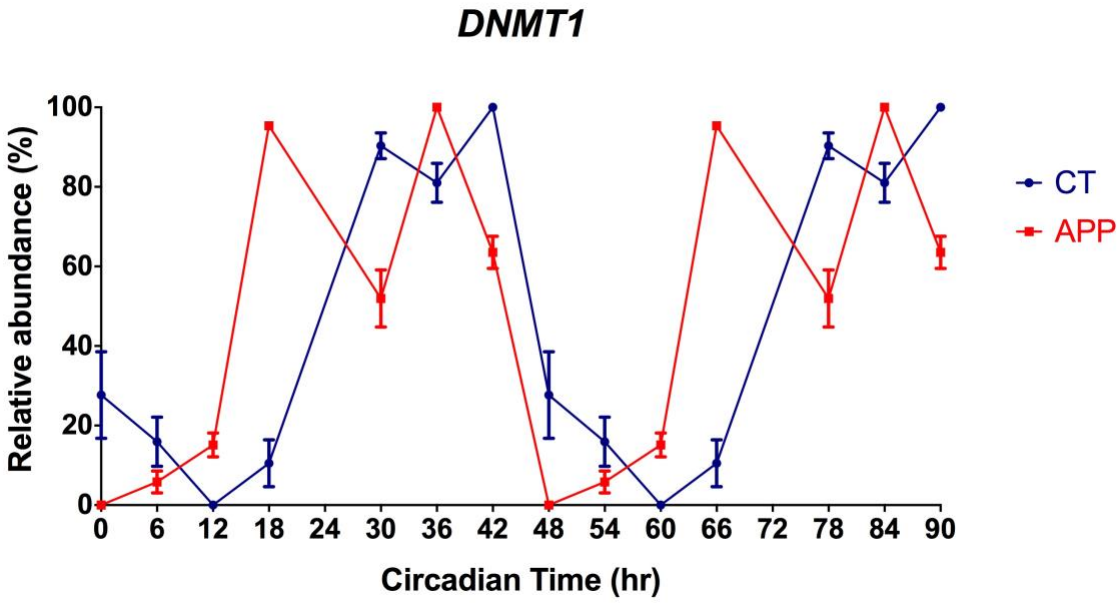

Figure 11. *Dnmt1* is expressed rhythmically in adult rat hippocampal (ARH) neurons and exhibits aberrant rhythmicity with APP-overexpression.
Real-time PCR to quantify relative abundance of *Dnmt1* in APP-overexpressing (APP) versus control (CT) ARH neurons over time. Relative abundance determined by assigning 100% abundance to the highest 1/ΔCt value. Graph shows raw data from a representative biological replicate.

A

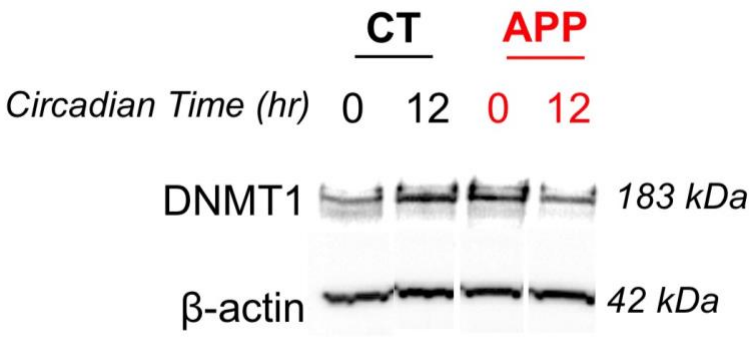

B

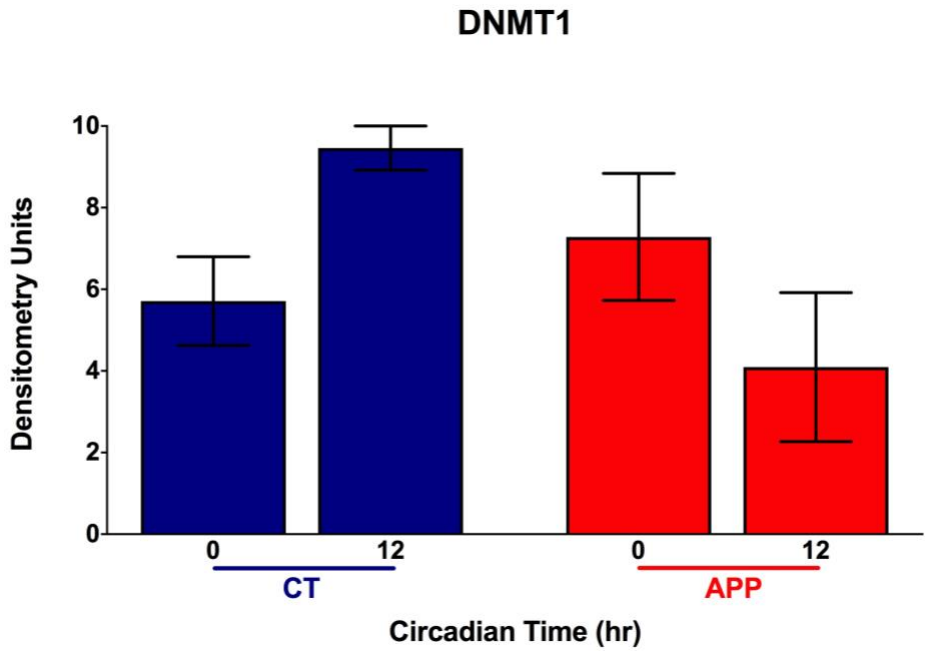

Figure 12. Dnmt1 protein levels are rhythmic in ARH neurons and Dnmt1 rhythmicity is altered with APP-overexpression.
A) Western Blot of protein extract from control (CT) versus APP-overexpressing (APP) ARH neurons, collected every 6 hours post synchronization. Blot was probed with antibody to visualize Dnmt1 (~183kDa). **B)** Densitometry to quantify Dnmt1 protein in Western Blot from *(B)*, and two other biological replicates at 0 and 12 hours post 36-hour synchronization (n=3).

ChIP-IT Assay: Bmal1 Binding to Dnmt1 Promoter

We aimed to investigate whether Bmal1 acts as a transcription factor regulation the temporal transcription of *Dnmt1* promoter and whether this regulation (if it occurs) is altered by APP-overexpression. Previous *in silico* analysis by our group identified 5 E-boxes – canonical binding sites for Bmal1 binding – on the proximal promoter of human *Dnmt1* (**Figure 13**). Similar analysis of the rat *Dnmt1* gene sequence – highly homologous to the human gene – identified 3 E-boxes in the proximal promoter region. To determine whether Bmal1 does indeed directly bind to *Dnmt1* promoter at these E-boxes, we performed a ChIP High Sensitivity assay in control and APP-overexpressing ARH neurons at different timepoints post synchronization (0 and 12 hours). Cross-linked and shreaded chromatin samples were immune-precipitated with an anti- Bmal1 antibody and the pooled factions were analyzed by qPCR for the enrichment of *Dnmt1* E-boxes 1-3. Additionally, fold enrichment of known Bmal1 targets *Per2* and *Dbp* [6], was also assessed in the Bmal1 immunoprecipitated chromatin as controls for the assay. Our results indicate that Bmal1 binds to *Dnmt1* E-boxes 1 and 2 at 12 hours in control ARH neurons, however not at 0 hours. In the control neurons, there was a 2 fold enrichment of *Dnmt1* E-box 1 and a 2.1 fold enrichment of *Dnmt1* E-box 2 at 12 hours (**Figure 14A**). Bmal1 did not bind to Dnmt1 E-box 3 (**Figure 14A**). In APP-overexpressing ARH neurons Bmal1 binding to *Dnmt1* E-box 1 was dampened at 12 hours, compared to control ARH neurons. However at 0 hours, Bmal1 binding to E-box 1 was increased in APP-overexpressing ARH neurons compared to control neurons (**Figure 14A**). Bmal1 binding to *Dnmt1* E-box 2 was obliterated in APP-overexpressing ARH neurons (**Figure 14A**). As expected, Bmal1 did bind to *Per2* temporally in control ARH neurons: a 3.2

fold enrichment was detected at 0 hours and a 6.6 fold enrichment was detected at 12 hours. In APP-overexpressing ARH neurons, however, a 4.4 fold enrichment was detected at 0 and a 3.8 fold enrichment was detected at 12 hours (**Figure 14B**). We also found temporal Bmal1 binding to *Dbp* in control ARH neurons: we detected a 2.3 fold enrichment at 0 and a 3.5 fold enrichment at 12 hours. However, in the APP-overexpressing ARH neurons Bmal1 was only bound to *Dbp* at 12 hours (**Figure 14C**).

A

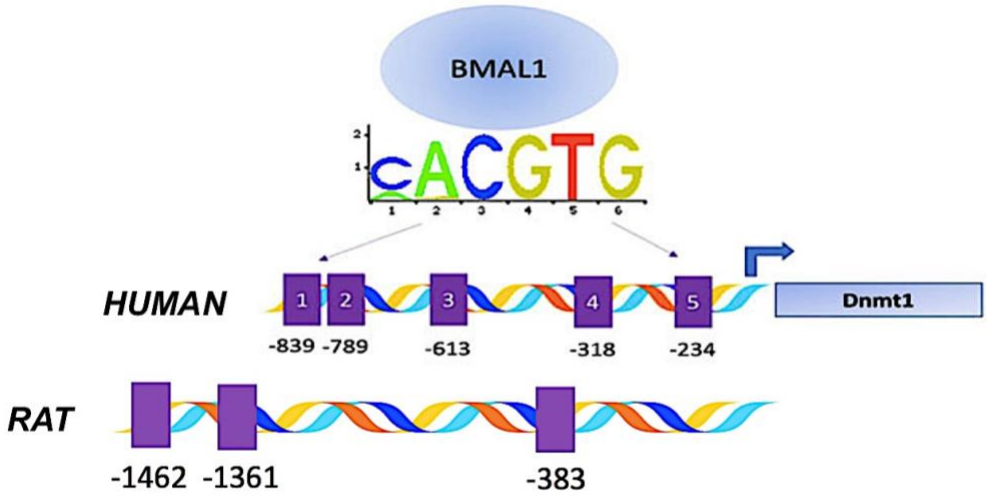

B

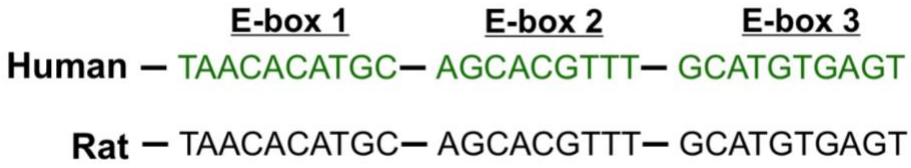

Figure 13. Hypothesized binding of Bmal1 to human and rat *Dnmt1* promoter. **A)** Schematic of hypothesized binding of Bmal1 to human and rat *Dnmt1* promoter. **B)** Sequences of E-boxes 1-3 on human and rat *Dnmt1* promoter.

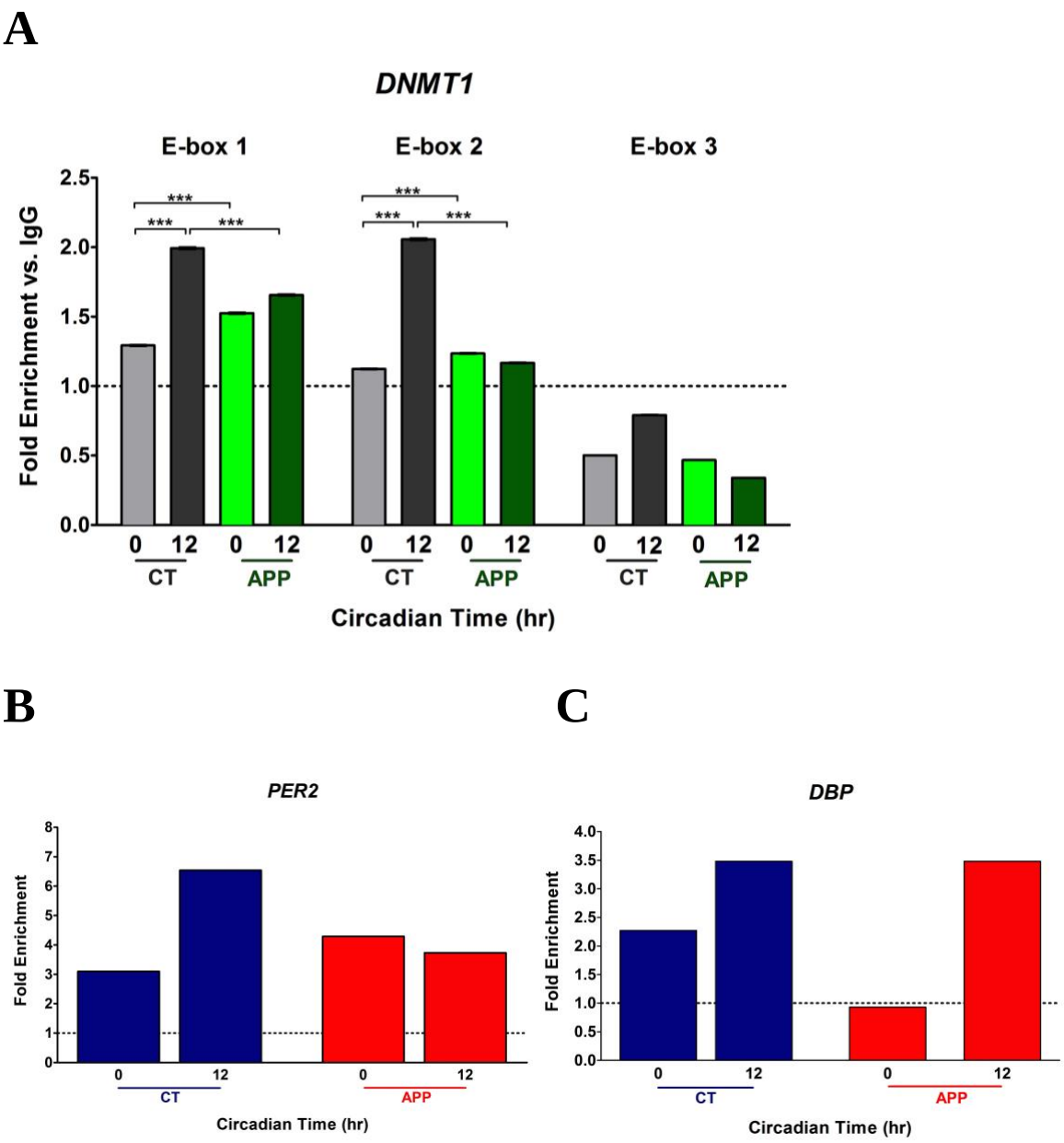

Figure 14. ChIP High Sensitivity Assay: Bmal1 rhythmically binds to E-boxes 1-2 on *Dnmt1* promoter and this binding is disrupted with APP overexpression.
A-C) Fold enrichment of control (CT) and APP-overexpressing (APP) adult rat hippocampal (ARH) neuron chromatin immunoprecipitated with Bmal1 antibody versus IgG antibody at 0 and 12 hours post synchronization. Fold enrichment greater than 1 indicates Bmal1 binding. Rat primers flanking E-boxes 1-3 on *Dnmt1* promoter (**A**), *Per2* promoter (**B**), and *Dbp* promoter (**C**) were used for real-time PCR.

DNMT1 in Bmal1 Knockout (Bmal1 KO) Fibroblasts

Overall, our results strongly suggest that Bmal1 acts as a positive regulator of *Dnmt1* expression in neurons, and that this regulatory mechanism is altered in AD cellular models. As further proof of this interaction, we examined how reduction of Bmal1 affects levels of Dnmt1. To that end, we established 4 fibroblast lines from Bmal1 knockout mice (Bmal1 KO fibroblasts) and assessed the levels of *Dnmt1* mRNA and protein, via qPCR and Western Blot, respectively. As expected, if Bmal1 is a functional regulator of *Dnmt1* expression: Bmal1 KO fibroblasts showed an 80% reduction in *Dnmt1* transcript levels in comparison to NIH3T3 fibroblasts (**Figure 15A**). Furthermore, *Dnmt1* levels were significantly correlated to Bmal1 abundance, with *Dnmt1* levels increasing and *Bmal1* levels increased (Pearson's r=0.922, pvalue=0.0026), (**Figure 15B**).

Furthermore, Dnmt1 protein levels were also significantly reduced in the Bmal1 KO fibroblasts when compared to control NIH3T3 cells (**Figure 16A**). Densitometry analysis of the Western Blot confirmed this reduction in Dnmt1: the Bmal1 KO fibroblasts had an 80% decrease in Dnmt1 protein compared to control fibroblasts (**Figure 16B**).

A

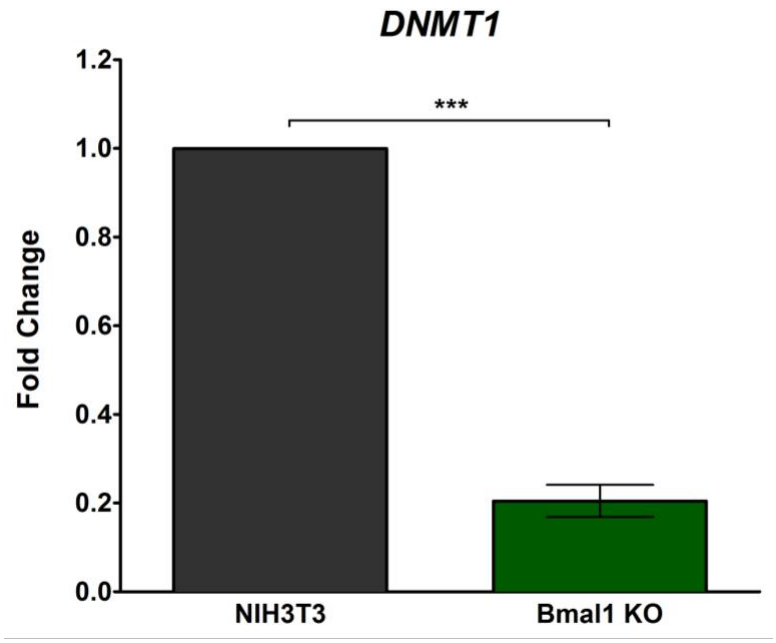

B

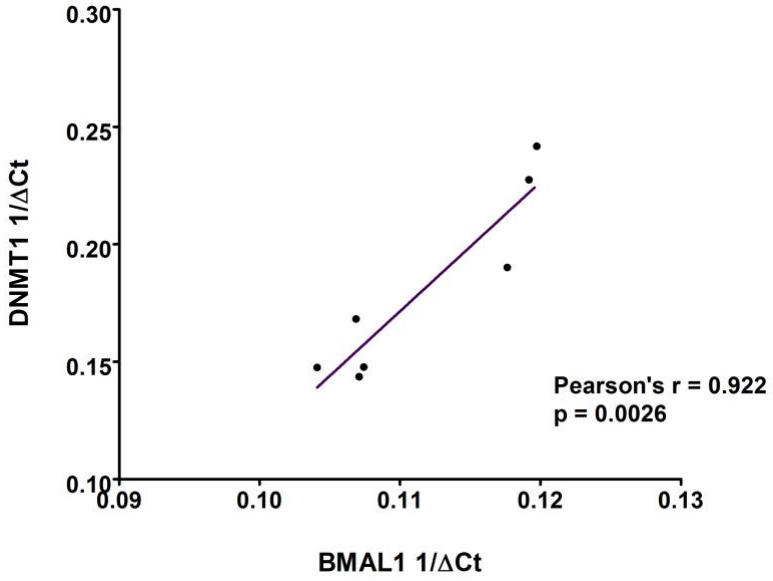

Figure 15. *Dnmt1* abundance in the Bmal1 knockout (Bmal1 KO) fibroblast line is decreased proportionally to decreasing Bmal1 levels.
A) Real-time PCR to quantify abundance of *Dnmt1* in Bmal1 KO fibroblasts. Fold change was calculated using NIH3T3 fibroblasts as control (p=0.0002 with n=4). **B)** Pearson's correlation of *Bmal1* and *Dnmt1* abundance in the Bmal1 KO fibroblasts (n=4).

A

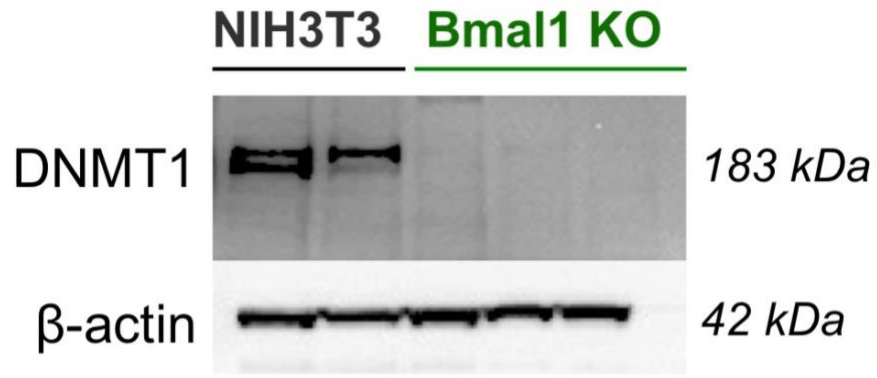

B

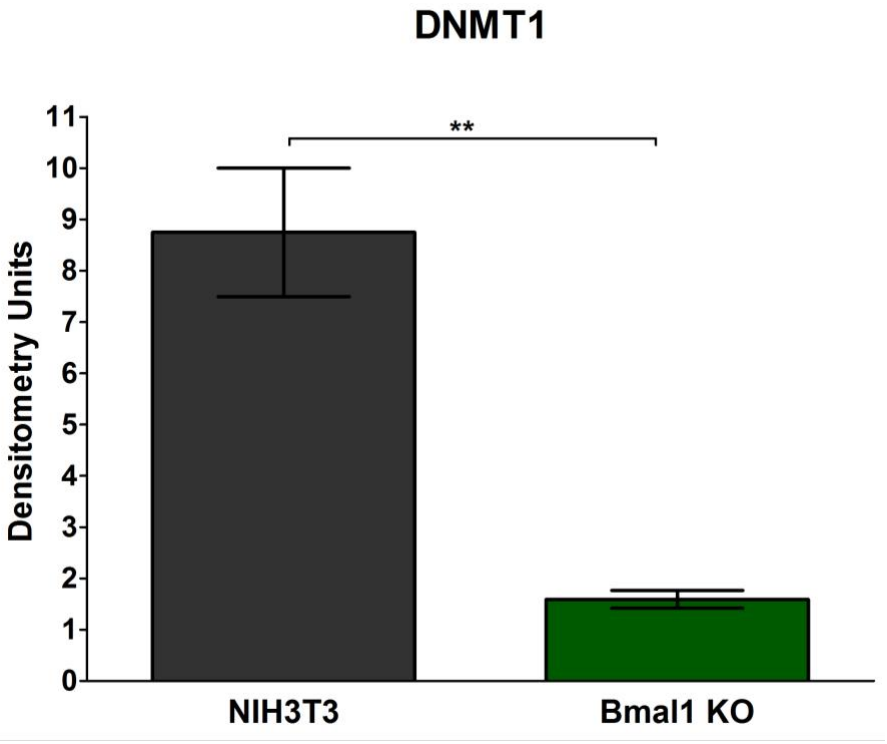

Figure 16. Dnmt1 protein levels are decreased in the Bmal1 knockout (Bmal1 KO) fibroblast line.
A) Western blot of protein isolated from Bmal1 KO fibroblasts and control NIH3T3 fibroblasts. Blot was probed with antibody to visualize Dnmt1 (~183kDa). **B)** Densitometry to quantify Dnmt1 protein in Western Blot from (A), with the two NIH3T3 lines grouped and the three Bmal1 KO fibroblast lines grouped ($p=0.005$ with $n=3$).

DISCUSSION

Our findings support direct, time-dependent circadian regulation of Dnmt1 – the most abundance enzyme that mediates DNA methylation in the adult brain – in hippocampal neurons, thus implicating circadian induced cycling of DNA methylation. Importantly, we also demonstrate significant alterations in this regulatory mechanism associated with Alzheimer's Disease pathology.

We examined the relationship between the circadian clock and DNA methylation in a neuronal, in vitro model of Alzheimer's Disease. Our AD model replicated the circadian deregulations previously reported in AD pathology; specifically, the circadian regulator Bmal1 exhibited aberrant rhythmicity upon accumulation of amyloid-β (**Figure 9-10**). This falls in line with previous studies that demonstrate altered oscillation of BMAL1, and other circadian clock genes, in AD brains [23, 27]. Moreover, neuronal model we generated in this study successfully processed and exported amyloid- β (**Figure 7-8**), thus further suggesting our Aβ involvement in mediating circadian alterations in AD [12].

In our study we demonstrate the cyclical, circadian-like expression of DNA methyltransferase 1, a key methylation catalyzer, in hippocampal neurons (**Figure 11-12**). Although 24-hour global DNA methylation rhythmicity has been previously reported in post-mortem, human prefrontal cortices [22], to our knowledge our study is the first to show circadian-like oscillation of any specific neuronal methyltransferase gene. We also demonstrate that Dnmt1's rhythmicity is aberrant upon amyloid-β accumulation (**Figure 11-12**), which strongly indicates the deregulatory role of AD pathology in DNA

methylation. This finding fits into previous studies that report epigenetic disruptions in AD. Alterations in DNA methylation have been reported in the frontal cortex and hippocampus of AD patients [28-30]. Cronin et.al (2016) showed that the 5'UTR region of *BMAL1*, specifically, is rhythmically methylated and that this rhythmicity is altered with AD pathology [23]. Taken together, these findings not only suggest that AD pathology disrupts rhythmic DNA methylation, but also indicate a potential cross-talk between the circadian clock and the DNA methylation machinery.

While Cronin et. al (2016)'s study supports epigenetic driven regulation of circadian genes, we demonstrate that there is also direct circadian regulation of DNA methylation. Specifically, the results of our ChIP assay show that Bmal1 acts as a rhythmic transcription factor that binds to *Dnmt1*'s promoter in a time-dependent manner (**Figure 14**). Furthermore, we also demonstrate that changes in Bmal1 abundance positively correlate with changes in Dnmt1 abundance (**Figure 15-16**), thus further supporting Bmal1's regulatory role in Dnmt1 expression. This regulatory relationship could explain, in part, the cyclical expression of Dnmt1 that we observed in hippocampal neurons: endogenous circadian regulator Bmal1 is expressed rhythmically and thus induces the rhythmic expression of Dnmt1. In our AD model, Bmal1 binding to *Dnmt1* promoter was dampened and the timing altered (**Figure 14**), thus supporting the changes in Dnmt1's rhythmic expression we observed in our APP-overexpressing ARH neurons (**Figure 11-12**). These findings suggest circadian clock deregulations as the drivers of the epigenetic alterations associated with AD pathology.

It was long hypothesized that dysregulation of the circadian clock is a downstream effect of AD pathology caused by the neurodegeneration in the

suprachaismatic nucleus, the main pacemaker of our biological rhythms [25]. However, recent studies have suggested that circadian deregulations actually contribute to AD related neurodegeneration [31-32]. For instance, epidemiological studies have demonstrated a correlation between fragmented sleep and loss of robust circadian rhythms in cognitively normal people with increased risk for developing dementia [33]. In the case of BMAL1 specifically, reduction or loss of BMAL1 has been show to increase expression of local apolipoprotein E (APOE), a high risk gene for genetically inherited AD [34]. Thus, it is possible that circadian deregulation occurs prior to the clinical manifestation of AD, especially considering that AD cognitive and behavioral impairments are known to occur decades after pathology onset [11]. In this case, early circadian alterations in AD could initiate the AD-associated changes in neuronal DNA methylation. Consequently, these changes in the rhythmicity of methylation machinery then further perpetuate aberrant circadian cycling (since DNA methylation, as previously discussed, is known to directly regulate expression of circadian genes such as BMAL1). However, further investigation is needed to confirm this causational role of the circadian clock in AD-associated epigenetic alterations. Regardless of this, our findings open up the potential of targeting the circadian clock in AD treatments or implementing circadian-related preventative therapy for high-risk AD patients to forestall onset of clinical symptoms. For instance, shifting the sleeping or feeding patterns of high-risk AD patients early in adulthood could potentially extend the time before cognitive and behavioral impairments occur.

It is important to note that our study had several limitations that would need to be addressed to produce a clear picture of the circadian and epigenetic mechanisms in AD

pathology. First, our work was conducted in an in vitro model of AD that, by nature, is not equivalent to in vivo AD pathology. While our APP-overexpressing cells did process and export amyloid-β, the extracellular Aβ plaques characteristic of AD could not accumulate in culture media. Furthermore, in the absence of other brain cells, particularly microglia, the chronic neuroinflammation stimuli could not be reproduced. In addition, our model only addresses one of the pathological cascades known to mediate AD: the amyloid-β; without yet testing for the effects of Tau hyperphosphorylation and accumulation in neurons. Future studies will be performed *in vivo* in mouse transgenic models of AD. In particular, we are starting the analysis of APP23, a model that overexpresses human APP carrying the Swedish mutation and shows amyloid pathology starting at 6 months of age. Importantly, this is the only transgenic mouse model of AD reported to exhibit circadian alterations, manifested by abnormal cage activity during the light phase and thus reminiscent of sundowning [37]. We will assess the oscilation of Dnmt1 in APP transgenic mouse brains from animals sacrificed every 6 hours. Furthermore, we would also like to conduct the ChIP assay in these brains to investigate the binding of Bmal1 to *Dnmt1 in vivo*. We anticipate that these studies will provide us with a more accurate representation of how BMAL1 regulates DNMT1 and impacts methylation and pathology in the context of AD. Moreover, it is important to note that our ChIP assay was done wit cells collected every 12 hours and was therefore limited in reproducing the entire circadian pattern of regulation. Our future studies *in vivo* will allow us to remedy this issue by lowering the time between sample collection from 12 to 6 hours.

Finally, although we demonstrated the oscillation, and temporal circadian regulation of Dnmt1 specifically, it is worthwhile to examine other methyltransferases, such as Dnmt3a and Dnmt3b, as well as demethylases, such as Ten-eleven-translocation dioxogenases (Tet1-3). Since cyclical methylation and demethylation have been reported in the brain – such as the rhythmic methylation of BMAL1 previously discussed [23] – it is likely that other methylation factors besides DNMT1 are playing a role in this methylation cycle. Furthermore, preliminary studies in our lab have found canonical binding sites for BMAL1 not only on the DNMT1 promoter, but also on the promoters of DNMT3a, DNMT3b, and via *in silico* analysis. We chose to investigate DNMT1 first for its high abundance in the human frontal cortex, however, given our findings, it will be significant to also examine the other DNMT genes and their TET counterparts.

In summary, our study demonstrated, for the first time, temporal regulation of DNA methylation enzymes by the circadian clock. Furthermore, we also show the disruption of this pathway in association with AD pathology, thus further elucidating the epigenetic and circadian deregulations that occur in AD. Mapping the way epigenetic and circadian mechanisms are affected by AD pathology will not only further our understanding of the molecular effects of this crippling illness, but also reveal potential therapeutic targets for AD treatment.

REFERENCES

[1] Querfurth HW, LaFerla FM. Alzheimer's disease. N Engl J Med 2010; 362:329–44.

[2]: Hebert LE, Scherr PA, Bienias JL, Bennett DA, Evans DA. Alzheimer Disease in the PopulationPrevalence Estimates Using the 2000 Census. *Arch Neurol.* 2003;60(8):1119-1122.

[3]: Levi F, Schibler U (2007). Circadian rhythms: mechanisms and therapeutic implications. *Annu Rev Pharmacol Toxicol***47**: 593–628

[4]: Nagoshi, E., Saini, C., Bauer, C., Laroche, T., Naef, F., & Schibler, U. (2004). Circadian Gene Expression in Individual FibroblastsCell-Autonomous and Self-Sustained Oscillators Pass Time to Daughter Cells. *Cell,119*(5), 693-705. doi:10.1016/s0092-8674(04)01054-2

[5]: Eckel-Mahan, K. L. (2012). Circadian Oscillations within the Hippocampus Support Memory Formation and Persistence. *Frontiers in Molecular Neuroscience,5*. doi:10.3389/fnmol.2012.00046

[6]: Takahashi, J. S. Transcriptional architecture of the mammalian circadian clock. *Nature Reviews Genetics***18,**164–179 (2016).

[7]: Yiannopoulou, K. G., & Papageorgiou, S. G. (2013). Current and future treatments for Alzheimer's disease. *Therapeutic Advances in Neurological Disorders*, *6*(1), 19–33

[8]: Trott, A. J., & Menet, J. S. (2018). Regulation of circadian clock transcriptional output by CLOCK:BMAL1. *PLOS Genetics,14*(1). doi:10.1371/journal.pgen.1007156

[9]: Hirtz D, Thurman DJ, Gwinn-Hardy K, Mohamed M, Chaudhuri AR, Zalutsky R. How common are the "common" neurologic disorders? Neurology 2007;68:326-337

[10] : Jilg, A., Lesny, S., Peruzki, N., Schwegler, H., Selbach, O., Dehghani, F., and Stehle, J. H. (2010). Temporal dynamics of mouse hippocampal clock gene expression support memory processing. *Hippocampus* 20, 377–388.

[11] : Goedert, M., & Spillantini, M. G. (2006). A Century of Alzheimers Disease. *Science,314*(5800), 777-781. doi:10.1126/science.1132814

[12]: Halliday, G., Robinson, S. R., Shepherd, C., & Kril, J. (2000). Alzheimers Disease And Inflammation: A Review Of Cellular And Therapeutic Mechanisms. *Clinical and Experimental Pharmacology and Physiology,27*(1-2), 1-8. doi:10.1046/j.1440-1681.2000.03200.x

[13]: Nelson, P. T., Alafuzoff, I., Bigio, E. H., Bouras, C., Braak, H., Cairns, N. J., Castellani, R. J., Crain, B. J., Davies, P., Del Tredici, K., Duyckaerts, C., Frosch, M. P., Haroutunian, V., Hof, P. R., Hulette, C. M., Hyman, B. T., Iwatsubo, T., Jellinger, K. A., Jicha, G. A., Kovari, E., Kukull, W. A., Leverenz, J. B., Love, S., Machenzie, I. R., Mann, D. M., Masliah, E., McKee, A. C., Montine, T. J., Morris, J. C., Schneider, J. A., Sonnen, J. A., Thal, D. R., Trojanowski, J. Q., Troncoso, J. C., Wisniewski, T., Woltjer, R. L., Beach, T. G. (2012). Correlation of Alzheimer Disease Neuropathologic Changes With Cognitive Status: A Review of the Literature. *Journal of Neuropathology & Experimental Neurology,71*(5), 362-381. doi:10.1097/nen.0b013e31825018f7

[14]***:*** Volicer, L., Harper, D. G., Manning, B. C., Goldstein, R., & Satlin, A. (2001). Sundowning and Circadian Rhythms in Alzheimer's Disease. *American Journal of Psychiatry,158*(5), 704-711.

[15]: Pollak CP, Perlick D. Sleep problems and institutionalization of the elderly. J Geriatr Psychiatry Neurol 1991;4:204–10.

[16]: Slats D, Claassen JA, Verbeek MM, Overeem S. Reciprocal interactions between sleep, circadian rhythms and Alzheimer's disease: focus on the role of hypocretin and melatonin. Ageing Res Rev 2013; 12:188–200.

[17]: Ripperger, J. A., & Merrow, M. (2011). Perfect timing: Epigenetic regulation of the circadian clock. *FEBS Letters,585*(10), 1406-141

[18]: J.P. Etchegaray , C. Lee , P.A. Wade , S.M. Reppert , Rhythmic histone acetylation underlies transcription in the mammalian circadian clock. *Nature*, **421**, (2003), 177– 182.

[19]: K. Bozek , A. Relogio , S.M. Kielbasa , M. Heine , C. Dame , A. Kramer , H. Herzel , Regulation of clock-controlled genes in mammals. *PLoS One*, **4**, (2009).

[20]: Y. Ji , Y. Qin , H. Shu , X. Li , Methylation analyses on promoters of mPer1, mPer2, and mCry1 during perinatal development. *Biochem. Biophys. Res. Commun.*, **391**, (2010), 1742– 1747.

[21]: Azzi, A., Dallmann, R., Casserly, A., Rehrauer, H., Patrignani, A., Maier, B., Kramer, A., Brown, S. A. (2014). Circadian behavior is light-reprogrammed by plastic DNA methylation. *Nature Neuroscience,17*(3), 377-382. doi:10.1038/nn.3651

[22]: Lim, A. S., Srivastava, G. P., Yu, L., Chibnik, L. B., Xu, J., Buchman, A. S., Schneider, J. A., Myers, A. J., Bennett, D. A., De Jager, P. L. (2014). 24-Hour Rhythms of DNA Methylation and Their Relation with Rhythms of RNA Expression in the Human Dorsolateral Prefrontal Cortex. *PLoS Genetics,10*(11). doi:10.1371/journal.pgen.1004792

[23]: Cronin, P., Mccarthy, M. J., Lim, A. S., Salmon, D. P., Galasko, D., Masliah, E., De Jager, P. L., Bennett, D. A., Desplats, P. (2016). Circadian alterations during early stages

of Alzheimer's disease are associated with aberrant cycles of DNA methylation in BMAL1. *Alzheimer's & Dementia*.

[24]: Chouliaras, L., Rutten, B. P., Kenis, G., Peerbooms, O., Visser, P. J., Verhey, F., van Os, J., Steinbusch, H. W., van den Hove, D. L. (2010). Epigenetic regulation in the pathophysiology of Alzheimers disease. *Progress in Neurobiology,90*(4), 498-510. doi:10.1016/j.pneurobio.2010.01.002

[25]: Stopa, E. G., Volicer, L., Kuo-Leblanc, V., Harper, D., Lathi, D., Tate, B., & Satlin, A. (1999). Pathologic Evaluation of the Human Suprachiasmatic Nucleus in Severe Dementia. *Journal of Neuropathology and Experimental Neurology,58*(1), 29-39. doi:10.1097/00005072-199901000-00004

[26]: Satlin, A., Volicer, L., Stopa, E. G., & Harper, D. (1995). Circadian locomotor activity and core-body temperature rhythms in Alzheimers disease. *Neurobiology of Aging,16*(5), 765-771. doi:10.1016/0197-4580(95)00059-n

[27]: Cermakian, N., Lamont, E. W., Boudreau, P., & Boivin, D. B. (2011). Circadian Clock Gene Expression in Brain Regions of Alzheimer ’s Disease Patients and Control Subjects. *Journal of Biological Rhythms,26*(2), 160-170. doi:10.1177/0748730410395732

[28]: Mastroeni D., Grover A., Delvaux E., Whiteside C., Coleman PD., Rogers J. Epigenetic mechanisms in Alzheimer's disease. *Neurobiol Aging.* 2011;32:1161–1180.

[29]: Bakulski, K. M., Dolinoy, D. C., Sartor, M. A., Paulson, H. L., Konen, J. R., Lieberman, A. P., Albin, R. L., Hu, H., Rozek, L. S. (2012). Genome-Wide DNA Methylation Differences Between Late-Onset Alzheimers Disease and Cognitively Normal Controls in Human Frontal Cortex. *Journal of Alzheimers Disease,29*(3), 571-588. doi:10.3233/jad-2012-111223

[30]: Chouliaras, L., Mastroeni, D., Delvaux, E., Grover, A., Kenis, G., Hof, P. R., Steinbusch, H. W., Coleman, P. D., Rutten, B. P., van den Hove, D. L. (2013). Consistent decrease in global DNA methylation and hydroxymethylation in the hippocampus of Alzheimers disease patients. *Neurobiology of Aging,34*(9), 2091-2099. doi:10.1016/j.neurobiolaging.2013.02.021

[31]: Musiek, E.S., and D.M. Holtzman. 2016. Mechanisms linking circadian clocks, sleep, and neurodegeneration. Science. 354:1004–1008. doi:10.1126/science.aah4968

[32]: Hastings, M.H., and M. Goedert. 2013. Circadian clocks and neurodegenerative diseases: time to aggregate? Curr. Opin. Neurobiol. 23:880–887. doi:10.1016/j.conb.2013.05.004

[33]: Lim, A.S., M. Kowgier, L. Yu, A.S. Buchman, and D.A. Bennett. 2013. Sleep Fragmentation and the Risk of Incident Alzheimer’s Disease and Cognitive Decline in Older Persons. Sleep (Basel). 36:1027–1032. doi:10.5665/sleep.2802

[34]: Kress, G. J., Liao, F., Dimitry, J., Cedeno, M. R., Fitzgerald, G. A., Holtzman, D. M., & Musiek, E. S. (2018). Regulation of amyloid-β dynamics and pathology by the circadian clock. *The Journal of Experimental Medicine*,*215*(4), 1059-1068. doi:10.1084/jem.20172347

[35] Khan, M., & Gasser, S. (2016). Generating Primary Fibroblast Cultures from Mouse Ear and Tail Tissues. *Journal of Visualized Experiments*,(107). doi:10.3791/53565

[36] Song, H., Moon, M., Choe, H. K., Han, D., Jang, C., Kim, A., Cho, S., Kim, K., Mook-Jung, I. (2015). Aβ-induced degradation of BMAL1 and CBP leads to circadian rhythm disruption in Alzheimer's disease. *Molecular Neurodegeneration*,*10*(1). doi:10.1186/s13024-015-0007-x

[37] Vloeberghs, E., Dam, D. V., Engelborghs, S., Nagels, G., Staufenbiel, M., & Deyn, P. P. (2004). P68 Altered Circadian Locomotor Activity In App23 Mice: A Model For Bpsd Disturbances. *Behavioural Pharmacology*,*15*(5). doi:10.1097/00008877-200409000-00108